



# Power Monitoring System using the Internet of Things for Photovoltaic Powered Fertigation System

Noor Syahirah Ahmad Safawi<sup>1</sup>, Ahmad Fateh Mohamad Nor<sup>1,2\*</sup>

<sup>1</sup>Department of Electrical Engineering, Faculty of Electrical and Electronic Engineering, Universiti Tun Hussein Onn Malaysia, Batu Pahat, 86400, MALAYSIA

<sup>2</sup>Green and Sustainable Energy Focus Group (GSEnergy), Faculty of Electrical and Electronic Engineering, Universiti Tun Hussein Onn Malaysia, Batu Pahat, 86400, MALAYSIA

\*Corresponding Author

DOI: <https://doi.org/10.30880/emait.2023.04.02.001>

Received 1 July 2023; Accepted 20 November 2023; Available online 31 December 2023

**Abstract:** This research paper explains the concept of photovoltaic (PV) systems. Among renewable energy technologies, PV systems rank third after hydropower and wind in terms of usage. They find significant application in agricultural activities, contributing to income generation for daily livelihoods. However, certain plant species demand meticulous attention to achieve optimal efficiency, necessitating a larger workforce for their care. By incorporating the Internet of Things (IoT), users gain the ability to remotely monitor PV system performance through a dedicated application. The central goal of this project involves crafting a simulation of an IoT system. This system is intended for monitoring the functionality of PV systems and devising an IoT-based model for overseeing the power aspects of PV systems in conjunction with fertigation systems (watering plants with nutrient solutions). A key feature of this system is its capacity to gauge the IoT model's effectiveness by contrasting outcomes derived from hands-on observation and simulated scenarios. The outcomes of this study reveal that the developed IoT system effectively tracks real-time parameters like current, voltage, generated power, and solar PV temperature. It successfully establishes a link between users and the IoT infrastructure for system monitoring. Looking ahead, the gathered PV output data will be instantly accessible on mobile devices. This empowers users to assess the performance of their PV systems concerning fertigation.

**Keywords:** Photovoltaic system, fertigation system, monitoring system, Internet of Things

## 1. Introduction

One of the vital resources for human existence is electrical energy, which is primarily derived from non-renewable sources. Since non-renewable resources like fossil fuels are almost exhausted, the cost of obtaining them will rise as they become more difficult to find [1]. Furthermore, the utilization of fossil fuels has environmental repercussions for the phenomenon of global warming. In practice, numerous farmers employed fuel resources to operate their farming machinery, including generators responsible for activating motor pumps [2]. This circumstance arises as a result of the difficulty in implementing the farm's electrical grid infrastructure [3].

Due to the problem, people are starting to get involved in PV solar industry. After hydropower and wind, the photovoltaic (PV) system is presently the third most widely used renewable energy technology. PV system generates the sun's energy and converts it to electrical energy due to its low cost and high efficiency. As there is more sunlight than rain in Malaysia, it is perfect for constructing a PV-powered fertigation system as it is clean and can be installed remotely [4], [5]. The primary objective of this undertaking is to develop a power monitoring solution utilizing the Internet of Things (IoT) for a photovoltaic-driven fertigation system, with a special emphasis on its applicability to

\*Corresponding author: [afateh@uthm.edu.my](mailto:afateh@uthm.edu.my)

farmers. IoT is used in this project because farmers will be more capable of monitoring the fertigation system even though they are far away. To make sure that the output of the PV system is smooth we need to use IoT to monitor the system. This is because many factors can be disturbances to the PV panels such as dust and animal waste that will interfere with the output of PV systems.

## 2. Materials and Methods

The approach to devising the power monitoring system, employing the Internet of Things for photovoltaic-powered fertigation systems, is elaborated through the integration of IoT technology.

### 2.1 Concept in Development of the Solar PV Monitoring System

This project aims to design and build a solar-powered automated system with IoT capabilities and a monitoring system. The system's functioning as a whole will be shown via the prototype. Designing the entire monitoring procedure for the powered fertigation system is the first crucial stage that needs to be completed before creating the monitoring system. This project employs a set of components, including solar panels, a solar charge controller, a battery, a water pump motor serving as the load, Durian Uno, an ESP8266 Microcontroller unit (MCU), voltage and current sensors, a dust sensor, a temperature sensor, an LDR sensor, and a PIR motion sensor. The block diagram of the IoT-based solar PV monitoring system is shown in Fig. 1.

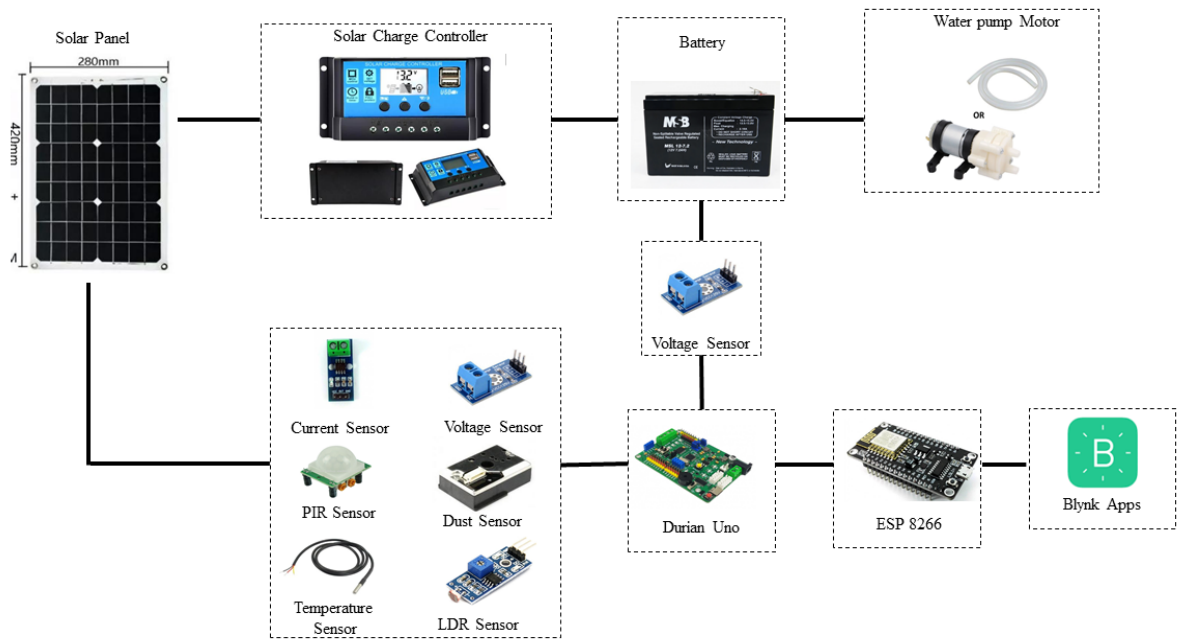


Fig. 1 - Block diagram of power monitoring system using IoT for photovoltaic powered fertigation system

### 2.2 Solar PV System Development

To prevent any harm to the system, including the main system and the connecting system of the solar sources, the photovoltaic system's design is crucial. Determining the estimated size of the solar system is therefore crucial before making any purchases or beginning a project. As illustrated in Fig. 2, several essential components must be measured in detail to make sure the solar system can support the entire project system: load sizing, solar sizing, battery sizing, and charger controller size.



Fig. 2 - The procedure for measuring an important component in the installation of solar panel

### 2.2.1 Load Calculation

To accurately determine the suitable dimensions for the solar panel, it is necessary to consider to think about the type of load the system will have to determine the proper solar panel sizing. The energy consumption is a crucial load metric. Hence, it is important to consider the load's power rating, the quantity of load utilization, and the daily operating hours as the essential specifications to be considered. Eq. 1 must be used to calculate a load's energy consumption [6].

$$E = P \times n \times h \tag{1}$$

Where n is the quantity of load used, P is the load's power rating, E is the daily energy consumption in Wh, and h is the load's operational hour per day. But the energy use must take into the energy wasted in a system. The equation for total consumption is shown in Eq. 2 [7].

$$E_T = E \times k_1 \tag{2}$$

Here,  $E_T$  represents the overall energy consumed daily, while  $k_1$  stands for the safety factor that accounts for losses.

### 2.2.2 Solar Sizing

This section will delve into the calculations for sizing the solar PV panel. Ensuring that the power generated by the PV panel can effectively supply the load is crucial, given the variation in PV panel sizes. Consequently, several factors must be ascertained. Primarily, it is necessary to establish the daily wattage consumption of the load. Additionally, the local climate in the installation area determines the daily minimum peak sun hours. The equation delineating the total wattage requisite for the PV panel is presented in Eq. 3 [7].

$$P_{PV} = \frac{E_T}{t_{min}} \tag{3}$$

In this context,  $P_{PV}$  represents the wattage necessary for the PV modules and signifies the minimum peak sun hours per day. Subsequently, the calculation process moves on to determining the quantity of PV panels necessary for the system. This computation involves utilizing the specifications of the PV panel to establish its maximum power output. The equation for figuring out how many PV panels are required for the system is shown in Eq. 4.

$$N_{PV} = \frac{P_{PV}}{P_{max(panel)}} \tag{4}$$

This equation represents the count of PV panels and signifies the maximum power generated by an individual PV panel.

### 2.2.3 Battery Sizing

When determining the appropriate battery size, it's essential to factor in the battery's autonomy days, which denotes the duration the battery can power the source before it depletes. Equation 5 provides the formula for calculating the battery's capacity in Ampere-hours (Ah) [7].

$$Battery\ Size\ (Ah) = \frac{E_i}{(EN \times DD \times NV)} \times Dof \tag{5}$$

Where is battery size capacity is in Ampere-Hours (Ah),  $E_i$  is the energy demand in watt-hours (Wh),  $Dof$  is the days of autonomy,  $NV$  is the nominal battery voltage,  $EN$  is the efficiency of the cable, battery, charge controller, and inverter and is the battery depth of discharge.

### 2.2.4 Charge Controller Sizing

A regulator known as the charge controller serves the purpose of restricting the current flowing from the PV panel to the battery. This component holds significant importance as it safeguards against both overcharging and excessive battery discharge, which could lead to a reduced lifespan. Essentially, charge controllers come in various types, differing in size, attributes, and their suitability for managing current. To accurately determine the appropriate size, Equation 6 provides a formula for acquiring a suitable current rating for the charge controller [7].

$$I_{rated} = I_{SC} \times N_{SP} \times K_{safe} \tag{6}$$

Where I is the rated current of the charger controller in Ampere (A),  $I_{SC}$  is the short circuit current of the solar panel,  $N_{SP}$  is the number connection of solar panel and the  $K_{safe}$  is the factor of safety in ensure that regulator can support the maximum current produced by the solar panel

### 2.3 Hardware Components and Software of the Designed System

Within this section, an enumeration and subsequent discourse of all the employed electronic components are presented. A total of thirteen (13) components will be incorporated to finalize the monitoring system, facilitating the collection of data aligned with the specified parameters.

#### 2.3.1 Solar PV Panel

In this endeavor, the prototype model utilizes an 18W aluminum substrate mono solar PV panel. The specifications for this solar panel are compiled and organized in Table 1.

**Table 1 - Specification of solar panel**

Features	Specification
Power	18W ± 5%
Size	420 x 280 x 2.5mm
DC Output	12V / 1.5A
USB Output	5V / 1.7A
Type	Mono Solar Panel
Material	Aluminum Substrate

#### 2.3.2 Solar Charge Controller

A solar charger controller, also known as a charge controller or solar regulator, is an essential component in a solar power system. Its main function is to regulate the flow of electric current between the solar panels and the battery bank to ensure safe and efficient charging. Table 2 is tabulated for the specification of the solar charge controller.

**Table 2 - Specification of solar charge controller**

Features	Specification
Charge Current	30A
Size	148.5 x 78 x 35mm
Voltage	DC 12V / 24V
Operating Temperature	-35~+60
Max Solar Input	12 V battery, highest 23V
Float Charge	13.7V
Discharge Stop	10.7V
Discharge Reconnect	12.6V
Charge Reconnect	13V

#### 2.3.3 Non-spillable Valve Regulated Sealed Rechargeable Lead Battery

The type of battery used in this project is an MSB 12V 7.2AH Non-Spillable Valve Regulated Sealed Rechargeable Lead Battery. This type of battery is usually used as a backup power and energy storage supply for many electrical devices. The battery is charged during the daytime using a solar panel, and the solar-charged controller will control the charging process. Table 3 is tabulated for the specification of the battery.

**Table 3 - Specification of battery**

Specification	MSB 12V 7.2AH
Battery Spec	12V 7.2AH
Boost / Equalize	4.5V – 15V
Float	13.5V – 13.8V
Max Charging Current	2.16A

### 2.3.4 Supplementary Hardware Components with Their Functions

In this project, a range of equipment and components are used to facilitate various functions and tasks. These components play crucial roles in the project's overall functionality and are integrated into the system seamlessly:

- **Durian Uno:** The Durian Uno is equipped with a USB connector and offers 16 analog input pins and 54 digital I/O ports, making it versatile for establishing connections with external devices. Among these 54 digital I/O ports, 14 pins can also be employed for generating PWM (Pulse Width Modulation) outputs. The wide input power supply range of DC 3.7V to 12V allows for the attachment of different types of batteries, such as AAx4 and a single 18650 Li-ion battery [8].
- **NodeMCU (ESP8266):** The NodeMCU, also known as the ESP8266, is a Wi-Fi microchip module that provides any microcontroller access to the Wi-Fi network.
- **Voltage Sensor:** A voltage sensor is utilized to gauge the value of the voltage supply. It employs the voltage divider principle, enabling the measurement of voltages that microcontrollers cannot sense using their analog inputs.
- **Current Sensor:** A current sensor, also known as a current transducer or current transformer, is employed to measure and monitor the flow of electric current in a circuit. It converts the current passing through a conductor into a proportional electrical signal for measurement and processing by other devices.
- **PIR Motion Sensor:** The Passive Infrared (PIR) sensor is used to detect the presence of animals based on changes in infrared radiation emitted by their bodies. PIR sensors are commonly employed in security systems, motion-activated lighting, and automation applications.
- **Temperature Sensor:** The DS18B20 Waterproof Temperature sensor is used to measure temperature. It utilizes a thermistor and capacitive moisture to measure the air temperature, transmitting a digital signal on the data pin connected to the Durian Uno [9].
- **Dust Sensor:** An optical dust sensor is employed to measure the density of dust accumulation on a surface. It requires a power supply of 7VDC and has minimal current consumption, drawing only 11mA.
- **LDR Sensor:** An LDR (Light Dependent Resistor) sensor is used to replace the solar irradiance sensor. LDR sensors are versatile and find applications in light sensing, automatic lighting control, and daylight harvesting. They detect and respond to changes in light levels.
- **DC Motor Water Pump:** A DC 12V water pump motor is used to drive water pumps that operate on a 12-volt direct current (DC) power source. It provides the necessary mechanical power to circulate or move fertilizer from the tank to the plant.
- **DC Motor 12V with Fans:** A DC 12V motor with fan blades is employed to generate airflow. This motor operates on a 12-volt direct current (DC) power supply and is commonly used in cooling systems, ventilation, and various air circulation applications.

### 2.4 Development of Solar PV Monitoring System Block Diagram

Based on Fig. 3, the central of the system is the microcontroller with Wi-Fi function enabled which is ESP8266. There are 6 types of inputs which are the voltage sensor, current sensor, temperature sensor, PIR sensor, Dust sensor, and LDR sensor. The sensor will be placed at different points of the junction box and the surface of the solar panel. The data accumulated by the sensors will be processed by the microcontroller and the output will be transmitted to the Blynk application for display purposes. These data can be transmitted over Wi-Fi as the microcontroller can be connected to the Wi-Fi. We will get to observe the real-time data and notification through the Blynk application. The accumulated data process can be seen in Fig. 4 to Fig. 9.

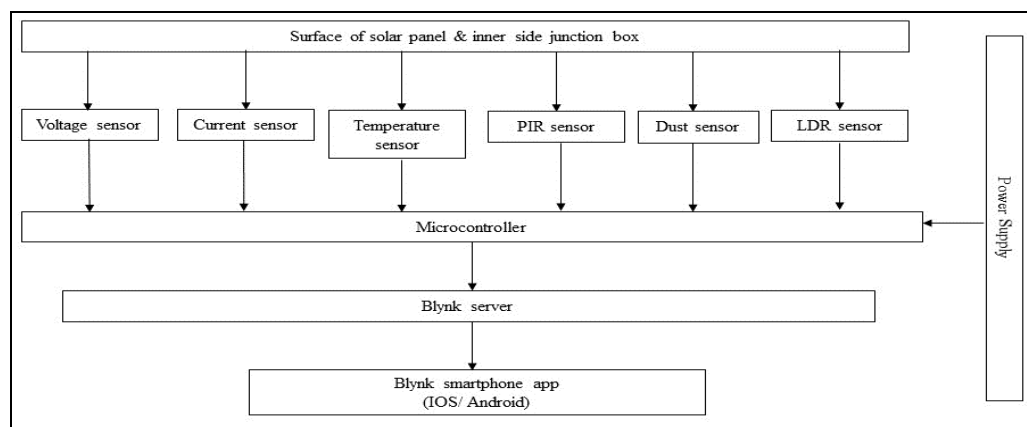


**Fig. 3 - Block diagram of the project**

### 2.4.1 Flow Chart of Voltage Sensor

The process will start with the hardware and software configuration. This will lead to the microcontroller programming and will be linked to the Blynk server. The hardware system will be triggered from the voltage sensor and the data will be accumulated and conveyed to the Blynk server. We are using the Durian Uno as the microcontroller and the data from the voltage sensor will be displayed in the Blynk application on the smartphone. If the reading of voltage from the sensor is more than 12V, we will get a notification from the Blynk application with the caption “Voltage Overload!”. The flow of the voltage sensor is shown in Fig. 4.

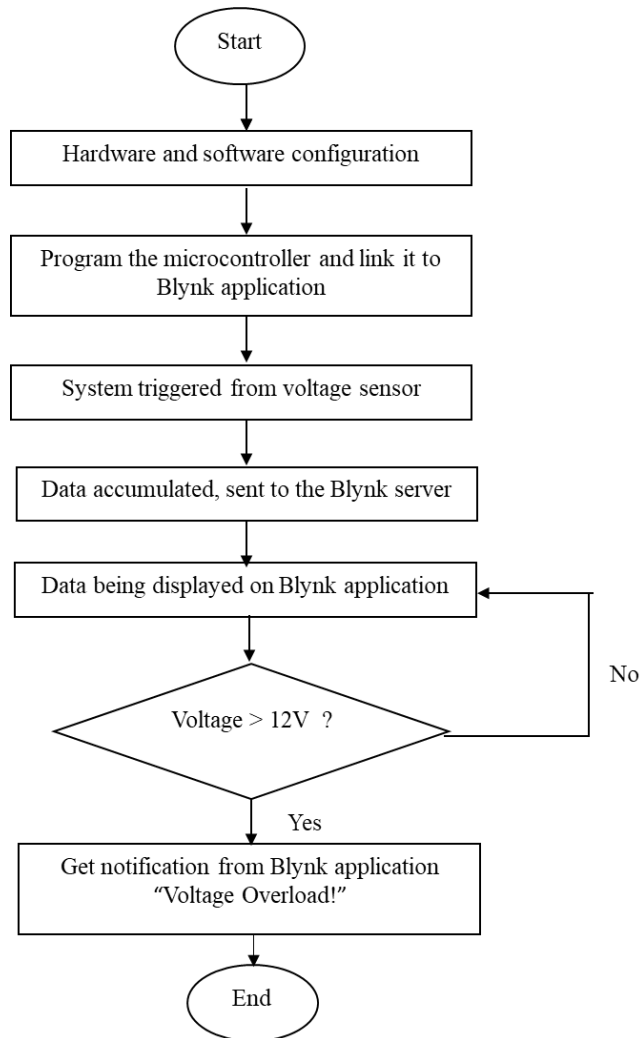
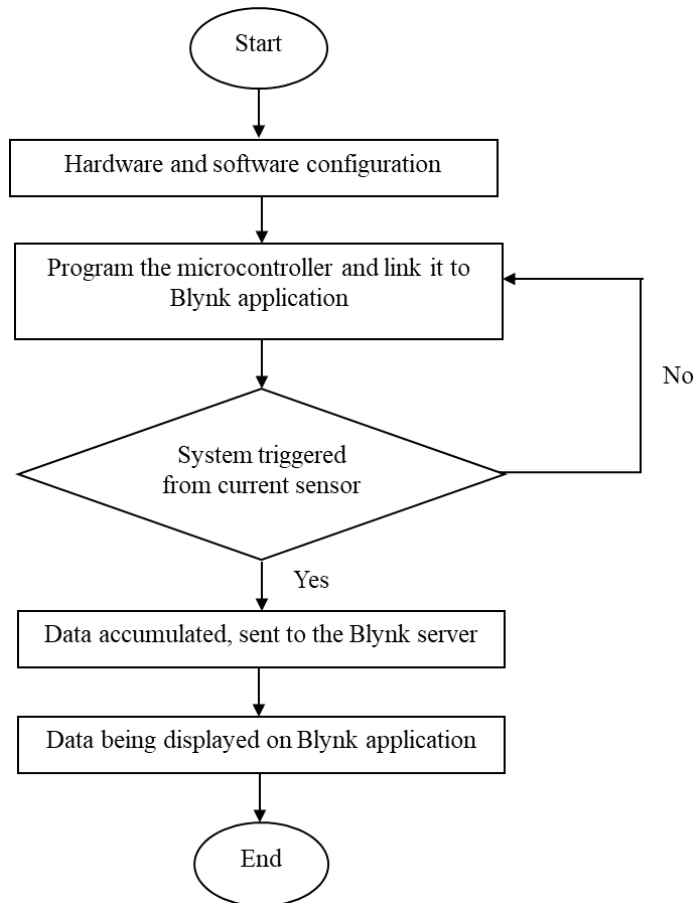


Fig. 4 - Flow chart of voltage sensor

### 2.4.2 Flow Chart of Current Sensor

Based on Fig. 5 the process will start with the hardware and software configuration. This will lead to the microcontroller programming and will be linked to the Blynk server. The hardware system will be triggered from the current sensor and the data will be accumulated and conveyed to the Blynk server. User can monitor the data displayed in real-time through their smartphone. The flow of the current sensor is shown in Fig. 5.



**Fig. 5 - Flow chart of current sensor**

### 2.4.3 Flow Chart of Temperature Sensor

Based on Fig. 6, the process will start with the hardware and software configuration. This will lead to the microcontroller programming and will be linked to the Blynk server. The hardware system will be triggered from the temperature sensor and the data will be accumulated and conveyed to the Blynk server. User can monitor the data displayed in real-time through their smartphone. The flow of the temperature sensor is shown in Fig. 6.

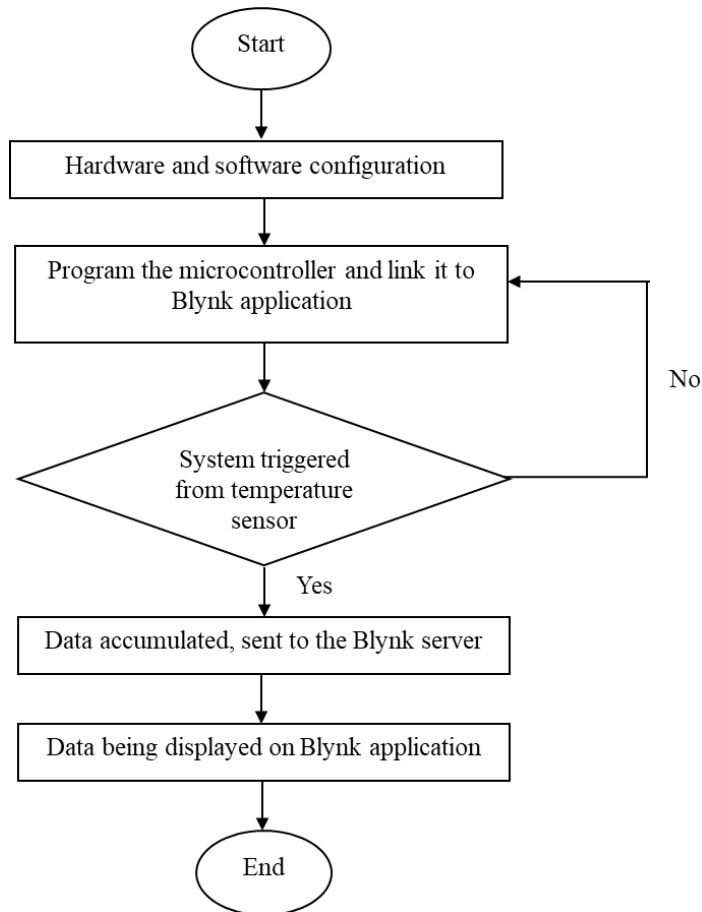


**Fig. 6 - Flow chart of temperature sensor**

### 2.4.4 Flow Chart of PIR Motion Sensor

Based on Fig. 7 the process will start with the hardware and software configuration. This will lead to the microcontroller programming and will be linked to the Blynk server. The hardware system will be triggered from the PIR motion sensor to trigger any motion from animals such as birds or monkeys and the data will be accumulated and conveyed to the Blynk server. User can monitor the data displayed in real-time through their smartphone. If the sensor detects any motion the switch in the Blynk application interface will change the colour to “RED” colour but if there is no motion detected the switch will be in “GREEN” colour. In addition, we will get a notification from the Blynk application with the caption “Motion Detected!” if detect any motion. Lastly, we can turn on or off the fan motor control in the Blynk application manually to drive away the animals from the solar panel because animals are sensitive to loud or sudden noises. The flow of the PIR motion sensor sensor is shown in Fig. 7.

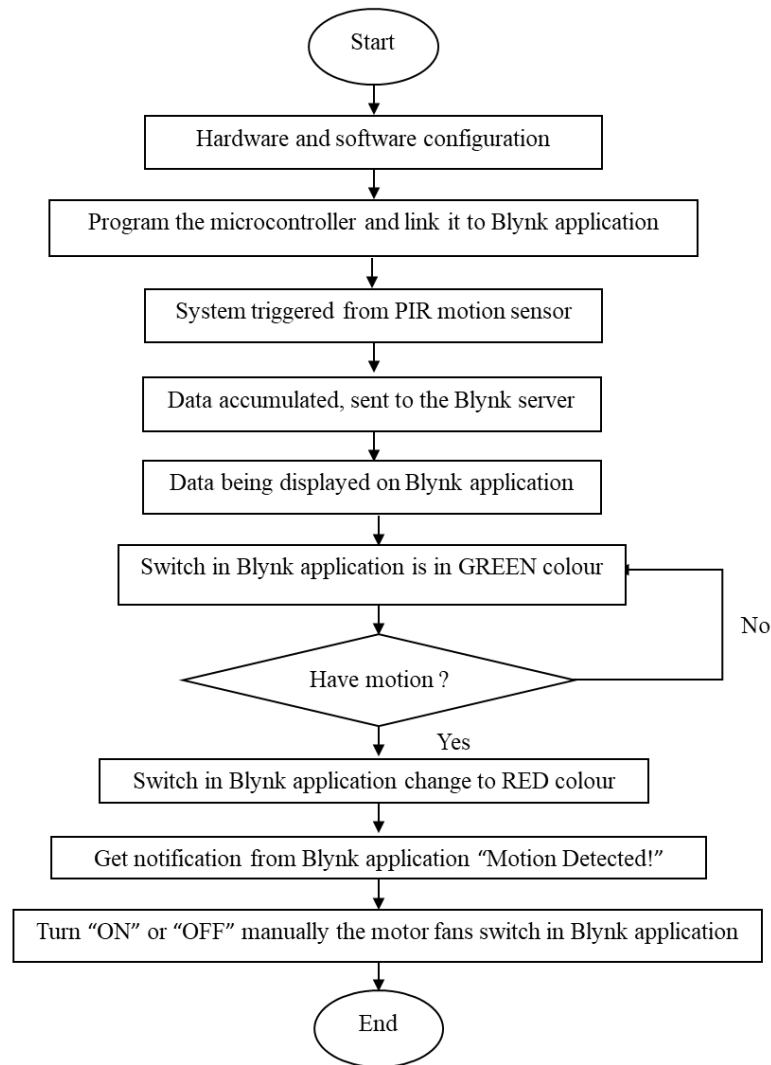


**Fig. 7 - Flow chart of PIR motion sensor**

### 2.4.5 Flow Chart of Dust Sensor

Based on Fig. 8 the process will start with the hardware and software configuration. This will lead to the microcontroller programming and will be linked to the Blynk server. The hardware system will be triggered from the dust sensor and the data will be accumulated and conveyed to the Blynk server. User can monitor the data displayed in real-time through their smartphone. The flow of the dust sensor is shown in Fig. 8.

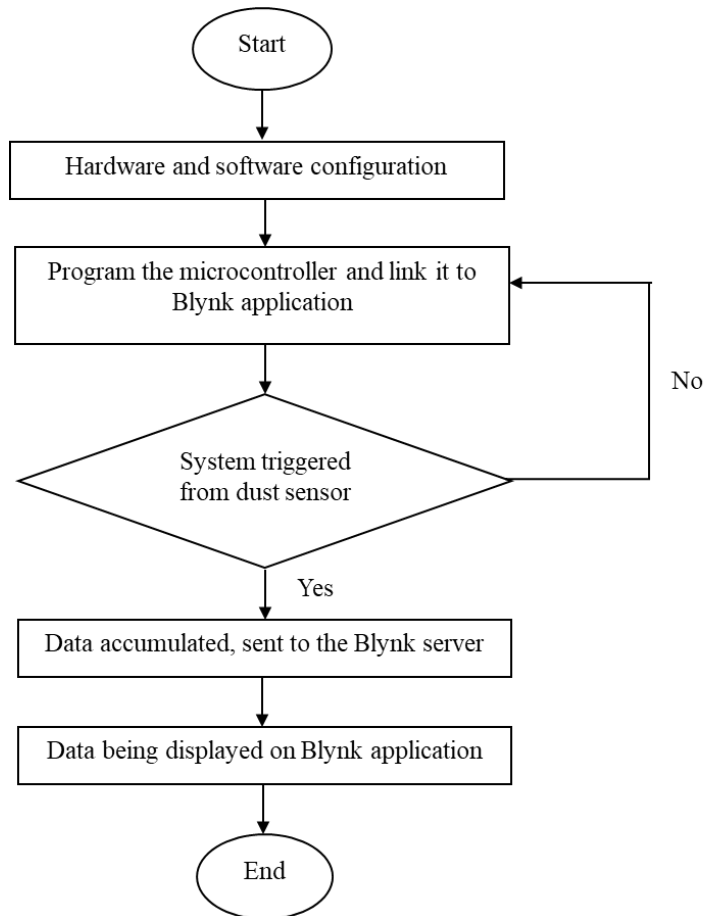


Fig. 8 - Flow chart of dust sensor

### 2.4.6 Flow Chart of LDR Sensor

Based on Fig. 9 the process will start with the hardware and software configuration. This will lead to the microcontroller programming and will be linked to the Blynk server. The hardware system will be triggered from the LDR sensor and the data will be accumulated and conveyed to the Blynk server. User can monitor the data displayed in real-time through their smartphone. The flow of the LDR sensor is shown in Fig. 4.

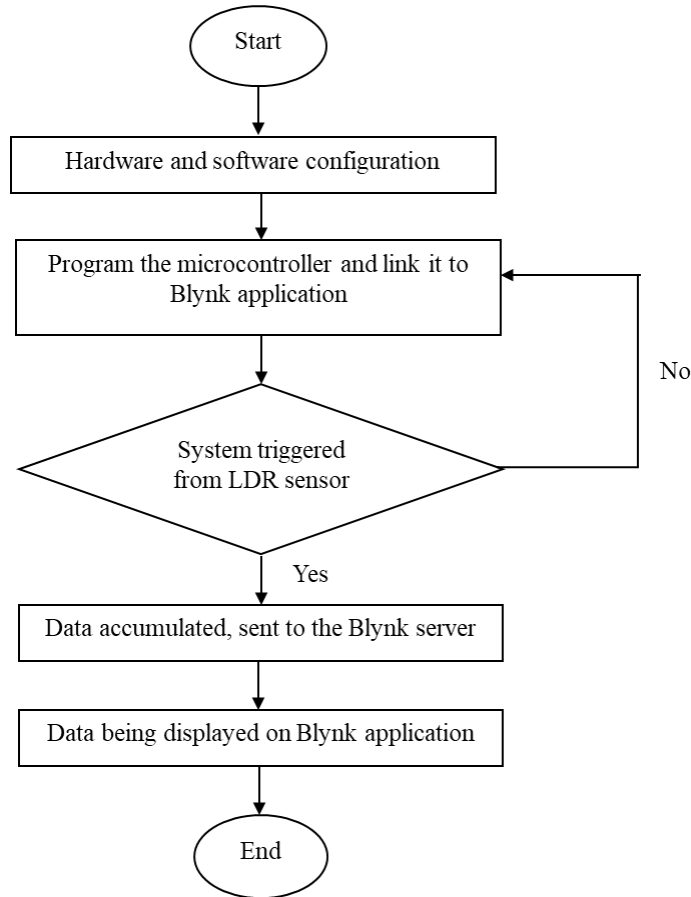


Fig. 9 - Flow chart of LDR sensor

## 2.5 Performance Evaluation of Solar Monitoring System

Several readings from the sensors were recorded, and the results of manual testing with a multimeter were compared to the readings to determine whether the system was functioning properly or not. Voltage, current, power, dust, temperature, and solar irradiance from the solar panel are the readings that are being taken. The testing was held from 14th June 2023 until 15th June 2023 at the front of the house in Taman Nusa Damai, Pasir Gudang. The testing was done 5 times a day.

### 2.5.1 Charge Controller Sizing

For this project, the calculation of the power value will be discussed. The formula to determine the percentage difference is shown in Eq. 7. The result of the calculation is shown in Table 6.

$$Power (P) = Voltage(V) \times Current (I) \tag{7}$$

The unit of power is measured in watts (W), where 1 watt is equal to 1 volt-ampere.

## 3. Results and Discussion

Within this segment, the acquired outcomes are subjected to discussion. The initial result encompasses the specifications of the Solar PV system within the Fertigation Sector. Subsequently, the second result encompasses both the hardware development and the simulation outcomes of the monitoring system. The third segment presents the data

monitoring process through two distinct methodologies. Lastly, the implementation of IoT through the Blynk application is addressed.

### 3.1 Solar PV System Design for a Real-life Case

The determination of the rating for each load is presented in Table 4, employing Equation 1 detailed in subsection 2.21. The motor pump operates for a duration of 0.25, equivalent to 15 minutes daily, due to the requirement of watering the plants five times a day, each time lasting 5 minutes.

**Table 4 - Rating of motor pump for fertigation system**

Load	Hp	Power (W)	Time used	Energy
Water Pump	0.5	0.373kW	0.25h	0.09325kWh

**Table 5 - Rating of solar panel system specification**

Item	Design value	Hardware Rating
Solar sizing	30.30 W	40 W
Battery capacity	54.85 Ah	55 Ah
Charge controller sizing	2.96 A	30 A

Based on the result in Table 5, it can be shown that the calculated is from the design value and the hardware rating is based on the approximately calculated value for the solar system. The solar panel will be 40W, and the battery will be 12V, 55AH with 3 days autonomy. The specifications of this battery allow it to last two days. Aside from that, the charge controller must be rated at 30A at 12V.

### 3.2 Circuit configuration of the solar monitoring system

In this part, all the sensors are integrated and linked to the Durian Uno microcontroller. To facilitate data transfer to the Blynk application, the NodeMCU is connected to the TX and RX pins of the Durian Uno. Consequently, the comprehensive configuration of the circuit connection is illustrated in Fig. 10.

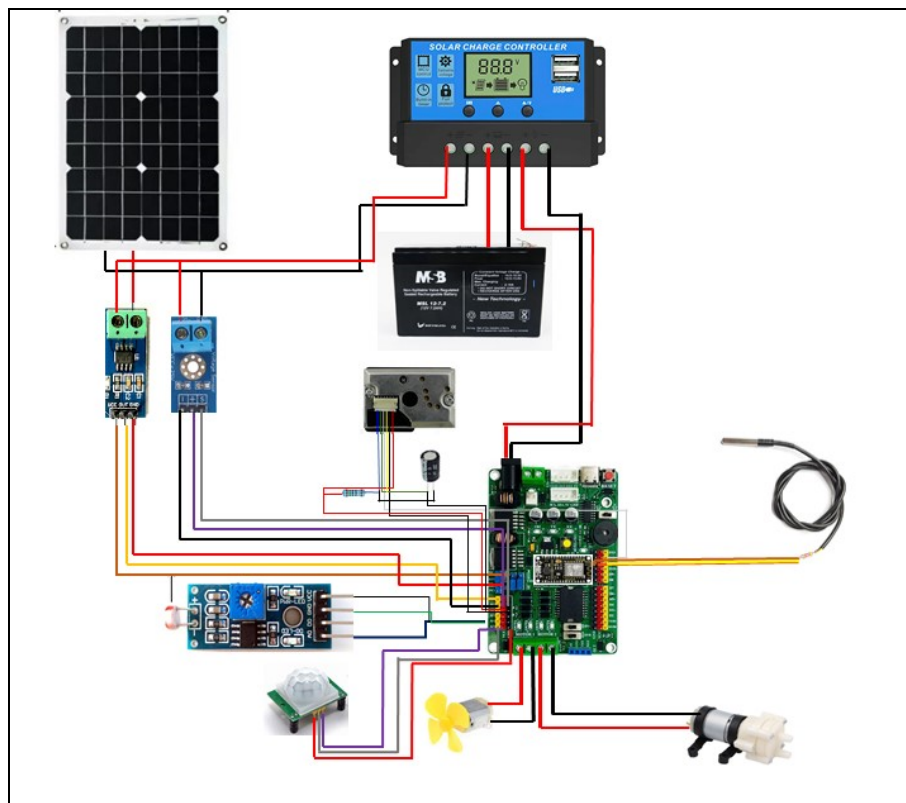


**Fig. 10 - Circuit of solar monitoring system**

In this case, when compared to the precise value of the system's power requirement, the prototype in this instance has an over specified design, as in Fig. 11, and Fig. 12, which also depicts the connection of the sensor and

microcontroller. This is so that money won't be wasted, and different components of this project can be utilized from earlier projects. This prototype's goal is to show how the system, which will be powered by a solar array, works conceptually and practically. Otherwise, this system was well-designed to prevent quickly harming the primary system of the fertigation component. The main controller of the fertigation system is powered by this solar system's specifications.

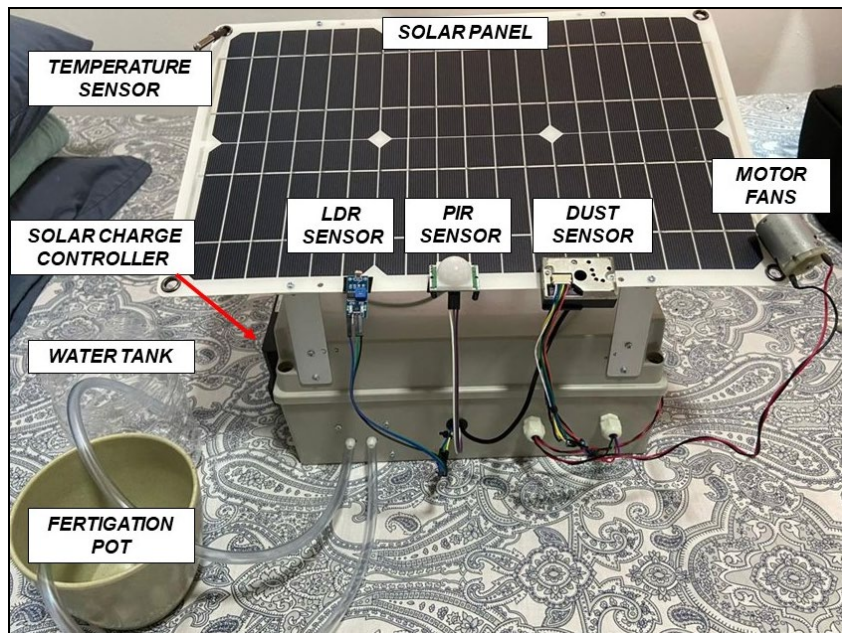


Fig. 11 - Prototype of solar monitoring system

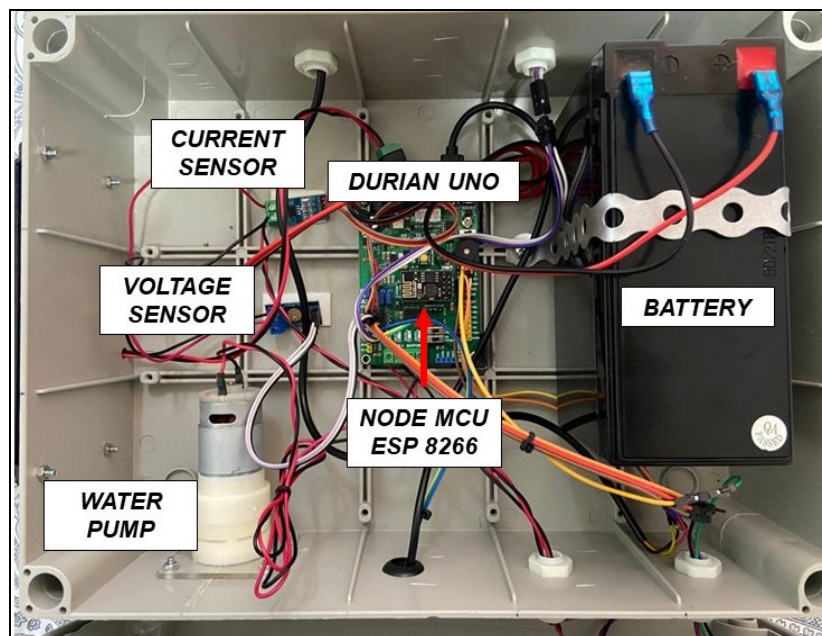


Fig. 12 - Component of hardware design

### 3.3 Performance of Solar Monitoring System

To verify the successful functionality of this system, a series of sensor readings were collected and cross-referenced with manual readings from a multimeter. The observed parameters included voltage, current, power, dust density, temperature, and solar irradiance generated by the solar panel. This testing phase occurred between June 14th and June 15th, 2023, situated in front of a residence in Taman Nusa Damai, Pasir Gudang. Conducted five times a day, the data displayed in Table 6 represents the values obtained from both sensors and the multimeter.

**Table 6 - Result of data obtained from sensor and multimeter**

Date & Time	Temperature (°C)	Reading from sensor			Reading from multimeter		
		Voltage (V)	Current (mA)	Power (W)	Voltage (V)	Current (mA)	Power (W)
14//6/2023 11.00 am	34.00	10.70	6.63	0.0709	10.74	8.50	0.0913
14/6/2023 11.30 am	35.00	10.80	6.26	0.0676	10.84	7.20	0.0780
14/6/2023 12.00 pm	37.60	10.00	9.37	0.0937	10.05	9.80	0.0985
14/6/2023 12.30 pm	38.50	10.20	8.48	0.0865	10.23	8.80	0.0900
14/6/2023 1.00 pm	41.00	10.70	6.26	0.0670	10.75	6.50	0.0699
15/6/2023 11.00 am	35.50	10.60	6.33	0.0671	10.62	6.70	0.0712
15/6/2023 11.30 am	37.19	10.91	6.18	0.0674	10.98	7.20	0.0791
15/6/2023 12.00 pm	37.90	10.80	6.18	0.0667	10.85	6.90	0.0749
15/6/2023 12.30 pm	39.00	10.77	6.33	0.0682	10.80	6.80	0.0734
15/6/2023 1.00 pm	37.00	10.50	6.26	0.0657	10.53	6.50	0.0684

Upon scrutinizing the outcomes provided in Table 6, noticeable discrepancies arise in the values of voltage, current, and power when comparing sensor readings with those from the multimeter. The percentage differences for these parameters are meticulously documented in Tables 7 to 9. To bolster the analytical assessment, graphical representations of the percentage differences in measurements for voltage, current, and power are presented in Fig. 13. To facilitate the analysis, Equation 8 lays out the formula employed to calculate the percentage difference. Within the equation, "Reading A" signifies the value derived from the sensors, while "Reading B" denotes the value obtained from the multimeter.

$$Percentage = \left| \frac{|Reading A| - |Reading B|}{\left(\frac{|Reading A| + |Reading B|}{2}\right)} \times 100\% \right| \tag{8}$$

where Reading A is the reading from the sensor and Reading B is the reading from the multimeter.

**Table 7 - The percentage of difference for voltage measurement**

Date & Time	Reading from sensor	Reading from multimeter	Difference percentage (%)
Voltage (V)			
14//6/2023 11.00 am	10.70	10.74	0.37
14/6/2023 11.30 am	10.80	10.84	0.37
14/6/2023 12.00 pm	10.00	10.05	0.50
14/6/2023 12.30 pm	10.20	10.23	0.30
14/6/2023 1.00 pm	10.70	10.75	0.47
15/6/2023 11.00 am	10.60	10.62	0.19
15/6/2023 11.30 am	10.91	10.98	0.64

15/6/2023 12.00 pm	10.80	10.85	0.46
15/6/2023 12.30 pm	10.77	10.80	0.28
15/6/2023 1.00 pm	10.50	10.53	0.29

**Table 8 - The percentage of difference for current measurement**

Date & Time	Reading from sensor	Reading from multimeter	Difference percentage (%)
Current (mA)			
14//6/2023 11.00 am	6.63	8.50	24.72
14/6/2023 11.30 am	6.26	7.20	13.97
14/6/2023 12.00 pm	9.37	9.80	4.49
14/6/2023 12.30 pm	8.48	8.80	3.70
14/6/2023 1.00 pm	6.26	6.50	3.76
15/6/2023 11.00 am	6.33	6.70	5.68
15/6/2023 11.30 am	6.18	7.20	15.25
15/6/2023 12.00 pm	6.18	6.90	11.01
15/6/2023 12.30 pm	6.33	6.80	7.16
15/6/2023 1.00 pm	6.26	6.50	3.76

**Table 9 - The percentage of difference for power measurement**

Date & Time	Reading from sensor	Reading from multimeter	Difference percentage (%)
Power (W)			
14//6/2023 11.00 am	0.0709	0.0913	25.15
14/6/2023 11.30 am	0.0676	0.0780	14.29
14/6/2023 12.00 pm	0.0937	0.0985	4.50
14/6/2023 12.30 pm	0.0865	0.0900	3.97
14/6/2023 1.00 pm	0.0670	0.0699	4.24
15/6/2023 11.00 am	0.0671	0.0712	5.93
15/6/2023 11.30 am	0.0674	0.0791	15.97
15/6/2023 12.00 pm	0.0667	0.0749	11.58
15/6/2023 12.30 pm	0.0682	0.0734	7.34
15/6/2023 1.00 pm	0.0657	0.0684	4.03

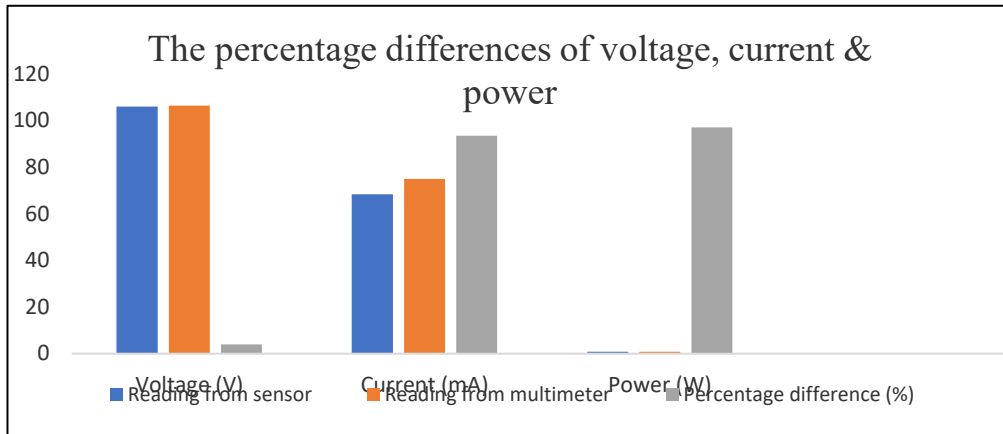


**Fig. 13 - The percentage differences in voltage, current, and power graph**

The voltage, current, and power are the three (3) variables that are determined for the percentage difference based on Tables 6 to 9. The percentage discrepancy between the voltage reading and the current and power readings, which range from 0.19% to 0.64%, is lower, proving that the voltage reading is accurate. The percentage disparities for reading current, with a range of 3.76% to 24.72%, however, exhibit the largest percentage, particularly during the early testing. Considering that the manual power calculation relies on current readings from a multimeter, the resulting percentage error in power readings is also notably substantial. The span of the percentage difference ranges from 3.97% to 25.15%.

Additionally, the multimeter computes average data and updates its display once every second. As a result, the sensors' readings have a minor variation. In the meantime, the sensor data is presented quickly and is updated every second. Since there is a chance that noise from the power supplies will cause the reading from the sensors to be higher or lower than the multimeters', this condition will have an impact on the reading.

Regarding the circuit connection, it's necessary to establish a series connection between the multimeter and the circuit to gather current data. Consequently, the data collection procedure can be susceptible to errors stemming from either human handling or instrument precision if the multimeter probes aren't securely attached to the solar panel's wiring. To mitigate such issues, using a clamp meter instead of a multimeter is recommended. Unlike multimeters, clamp meters do not require probe attachments for current measurements. Nevertheless, due to the relatively small magnitude of current in this prototype system, the clamp meter encounters challenges and inaccuracies when measuring minute values, particularly in the range of milliamperes (mA).

### 3.4 The Implementation of IoT for Monitoring System

In this section, the Blynk application serves as the platform to exhibit readings from all sensor types employed in the project, including voltage, current, power, temperature, dust density, light intensity, motion detection, motor fan control, and water pump status. This visual presentation is depicted in Fig. 14. This integration streamlines the monitoring process, eliminating the need for manual oversight. Personnel do not have to visit the farm daily for performance assessment of the solar system and plant health. The transmission of data from the Durian Uno to the NodeMCU (ESP8266) follows the same pattern, introducing a slight 1-second delay. This deliberate delay ensures that real-time data is promptly displayed for monitoring purposes. For voltage in this system, the max reading value for voltage is 20V when it's more than the stated value a notification will get from the Blynk application with the caption "Voltage overload!" as shown in Fig. 15.

In addition, the function of the PIR (Passive Infrared) sensor in this system is a device commonly used in security systems and lighting applications to detect the presence of animal movement such as birds or monkeys. When the PIR sensor detects the motion, the PIR status in the Blynk application will switch color of status from green to red and a notification is sent to the Blynk application with a caption of "Motion detected!" as shown in Fig. 16 and we can turn on or off the fans motor control in Blynk application manually to drive away the animals from the solar panel because animals are sensitive to loud or sudden noises. The role of the dust sensor within this system is to demonstrate the correlation between dust accumulation on the solar panel's surface and its subsequent influence on voltage, current, and power readings. This relationship stems from the fact that dust restricts the solar panel's exposure to sunlight irradiance. Additionally, the Blynk application visually displays the status of the water pump, indicating whether it's currently operating or not.



**Fig. 14 - The interface of the solar monitoring system through the Blynk application**

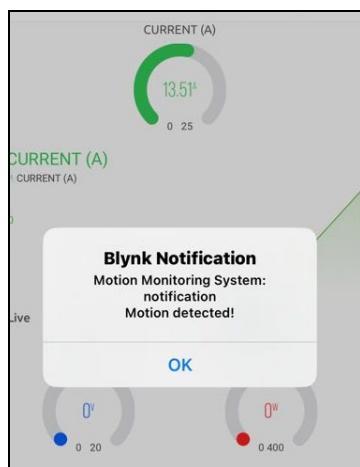


**Fig. 15 - The notification alert when voltage is more than 20V**

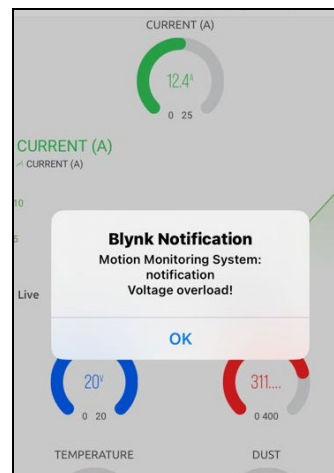


**Fig. 16 - The notification alert when PIR motion sensor detect motion**

#### 4. Conclusion

In conclusion, the use of this system and its basic design have demonstrated when the central controller can be powered by the solar power system. With the data gathered and the automated system's monitoring capability to switch from traditional to modern irrigation methods, it can be said that this project system has been functioning properly. When compared to conventional use, the plant's output may aid in ensuring that it receives the right nutrients to generate the best goods. Solar energy is a good example of how clean energy can help individuals save money on their monthly bills and reduce pollution. Several improvements need to be made for future studies based on the findings of this project studies:

- To enhance the accuracy of solar irradiance data, alternative sensors can be explored to ensure better measurements.
- It is recommended in the future to design the circuit on a Printed Circuit Board (PCB) to facilitate seamless connections between the sensor and the microcontroller.
- protection devices such as MCB and SPD can be added in the prototype design regarding their suitable limitation of voltage and current in helping to protect the system from damage because of the instability of power sources.

## Acknowledgement

The authors would like to thank the Faculty of Electrical and Electronic Engineering, Universiti Tun Hussein Onn Malaysia for its support.

## References

- [1] A. del Amo *et al.*, "An innovative urban energy system constituted by a photovoltaic/thermal hybrid solar installation: Design, simulation and monitoring," *Appl. Energy*, vol. 186, pp. 140–151, 2017.
- [2] FoodPrint, "How Our Food System Affects Climate Change," *Foodprint.org*, 2019.  
<https://foodprint.org/issues/how-our-food-system-affects-climate-change>.
- [3] M. N. Abdullah and I. Sapuan, "Stand-alone Solar Monitoring System using Internet of Things for Fertigation System," *Evol. Electr. Electron. Eng.*, vol. 1, no. 1, pp. 106–115, 2020.
- [4] S. A. Arefifar *et al.*, "Improving solar power PV plants using multivariate design optimization," *IEEE J. Emerg. Sel. Top. Power Electron.*, vol. 5, no. 2, pp. 638–650, 2017.
- [5] N. Mohd Ariff *et al.*, "Clustering of rainfall distribution patterns in peninsular Malaysia using Time Series Clustering Method," *Malaysian J. Sci.*, vol. 38, no. Special Issue 2, pp. 84–99, 2019.
- [6] A. N. Al-shamani *et al.*, "Design & sizing of stand-alone solar power systems a house Iraq," in *Recent Advances in Renewable Energy Sources*, 2013, pp. 145–150.
- [7] Levent Bas, "How to Size a Charge Controller," *Greentech Renewables*, 2010.  
<https://www.greentechrenewables.com/article/how-size-charge-controller>.
- [8] Mybotic, "Arduino STEM RBT project: Arduino Durian UNO ESP8266 IOT Starter Kit - Simplify IOT Project with Blynk," *MYBOTIC*, 2023.  
[https://mybotic.com.my/index.php?route=product/product&product\\_id=3743&search=ESP&page=2](https://mybotic.com.my/index.php?route=product/product&product_id=3743&search=ESP&page=2)
- [9] Y. S. Parihar, "Internet of Things and Nodemcu: A review of use of Nodemcu ESP8266 in IoT products," *J. Emerg. Technol. Innov. Res.*, vol. 6, no. 6, pp. 1085–1088, 2019.